

PACS numbers: 42.55.Lt; 42.60.By; 42.60.Da; 52.80.Pi
DOI: 10.1070/QE2006v036n07ABEH013201

RF-excited unstable-resonator planar CO_2 laser on all-metal electrode – waveguide structure

A.P. Mineev, S.M. Nefedov, P.P. Pashinin

***Abstract*. The radiation characteristics of a planar CO_2 laser excited by a diffusion-cooled rf discharge at a frequency of 40 MHz are studied. A single-mode cw lasing power of $\sim$50 W is achieved with an efficiency of $\sim$10 % for a nearly diffraction-limited radiation divergence of 4 – 7 mrad. The spatial structure, output power, stability and laser radiation quality are studied as functions of longitudinal and angular alignments of the resonator mirror for two types of hybrid unstable-waveguide resonators of the laser. It is shown that for the resonator corresponding to the negative branch of the stability diagram, a misalignment of 0.02 rad of the mirrors leads to a 50 % decrease in the output laser power, while its value for the positive branch resonator is about 100 times smaller. It is found that for the resonator corresponding to the negative branch, the sensitivity to the violation of confocal arrangement of the mirrors upon an increase in the resonator length is an order of magnitude higher. The dependence of the density of input rf power on the working gas pressure is studied experimentally in the interval 50 – 110 Torr. Power density values of 1 – 4 W cm^{-2} are obtained for normal discharge current density. These values are important for optimisation and scaling of the lasing characteristics of high-power planar CO_2 lasers.**

Keywords: *planar waveguide CO_2 laser, rf discharge, confocal waveguide-unstable hybrid resonator.*

1. Introduction

Planar waveguide carbon dioxide gas lasers (CO_2 PWL) excited by a diffusion-cooled radio-frequency (rf) discharge (without a cumbersome system of working gas circulation) attract great attention of researchers engaged in developing a new generation of inexpensive compact sealed gas-discharge cw and repetitively-pulsed kilowatt lasers with a high quality of optical radiation [1 – 9].

As a rule, the planar electrode – waveguide discharge system in such lasers is formed by two water-cooled metal electrodes with a high-quality finish of the working surfaces, which are either confined by one or two insulating side walls, or do not have any walls at all. This system is a modification of the rectangular waveguide in which one of the sides in the cross section is small (1 – 3 mm) and ensures an efficient diffusion cooling of the gas discharge plasma, while the other side is varied over a fairly wide range, thus ensuring a scaling of the area (and volume) of the active laser medium (based on the condition of attaining the required output power) and, if required, maintaining a constant length of the laser. Note that the planar structure envisages planar as well as profiled slotted discharge forms. Coaxial discharge can also be considered as a variety of a folded planar structure.

Uniform excitation of wide-aperture and extended active medium regions of such lasers can be provided due to the peculiarities of the spatial structure of transverse rf discharge in the frequency range 10 – 150 MHz. Such a discharge is highly stable to transitions from the volume regime to the constricted regime with increasing the working gas pressure (more than 100 Torr) and the specific energy input to the discharge plasma (more than 100 W cm^{-3}). The multitude of designs employed for realising transverse rf discharge and the ensuing possibilities of cw and pulse-periodic laser modes with a pulse repetition rate of tens of kilohertz are also worth mentioning.

As far as the design of the optical resonator for planar lasers is concerned, light fields with a high spatial coherence can be excited by using single-pass or multipass schemes. It is worthwhile to mention the hybrid waveguide-unstable confocal resonator with a unilateral extraction of optical radiation which can be used in an rf-excited cw CO_2 PWL to attain an output power of more than 1 kW in single-mode operation with a high quality of the laser beam having a divergence close to the diffraction limit [2].

However, all the advantages of the CO_2 PWL can be realised only for a complete and meticulous optimisation of the parameters of the gas-discharge active medium, as well as an appropriate choice of design for the electrode – waveguide discharge system and the optical resonator scheme, which determine the energy and spatial parameters of the laser radiation. In spite of the large number of publications devoted to the development and investigation of PWL, the optimisation of the working parameters of such lasers and their lasing parameters are still far from completion and require further investigations.

In this connection, we set out to develop a CO_2 PWL with a completely metal (without any insulating lateral walls) electrode – waveguide structure and carry out experimental studies and numerical simulation of laser radiation

A.P. Mineev, S.M. Nefedov, P.P. Pashinin A.M. Prokhorov General Physics Institute, Russian Academy of Sciences, ul. Vavilova 38, 119991 Moscow, Russia; e-mail: mineev@kapella.gpi.ru

Received 20 April 2006
Kvantovaya Elektronika **36** (7) 656 – 663 (2006)
Translated by Ram Wadhwa

parameters as functions of the exciting rf discharge parameters like the gas pressure, specific energy input and the input power. Due attention was also paid to the choice of the type and parameters of various schemes of hybrid waveguide-unstable optical resonator of the laser, and to the optimisation of these parameters and investigations of their effect on the energy and spatial parameters of laser radiation. Moreover, we also carried out detailed studies and comparison of the characteristics of the spatial modal structure, output power, stability and quality of laser radiation depending on the longitudinal and angular alignment of the resonator mirrors for two types of resonators. The electrical characteristics of the discharge, parameters and conditions of its operation in the laser channel were also studied. Knowledge of these parameters and conditions goes a long way in solving the problem of optimising the rf pumping and output parameters of lasers.

2. Design of the planar laser

Figure 1 shows the scheme of a planar CO_2 laser. The all-metal (without any insulating lateral walls) electrode–waveguide structure was formed by running-water-cooled aluminium electrodes whose surfaces were polished to a high quality and had a size 40×400 mm each. The discharge cross section was rectangular with sides $2b = 3$ mm (electrode gap) and $2a = 40$ mm.

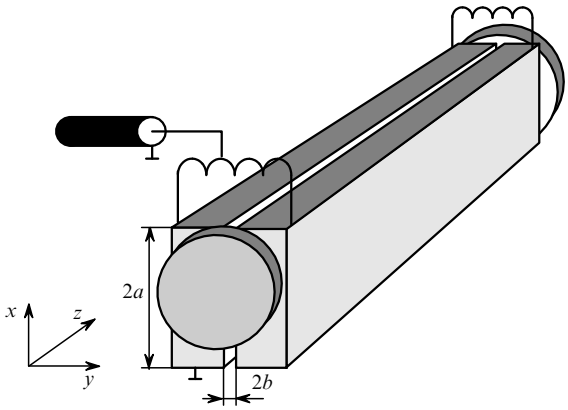

Figure 1. Scheme of a planar CO_2 laser. The size of the working surface of water-cooled electrodes is 40×400 mm. The interelectrode gap is 3 mm.

The electrode–waveguide structure was placed in a 580-mm long quartz tube with an inner diameter of 110 mm with its ends sealed hermetically to metal flanges with the help of rubber gaskets. The aligning components for the optical resonator mirrors were rigidly fastened to the quartz tube flanges and fixed with the help of four invar springs.

The rf power was supplied from one end of the electrodes through discharge load impedance matching device and an rf generator with an impedance of 50 Ω and a maximum output power of 600 W at a frequency of 40 MHz. The L-shaped matching device was formed by two inductances whose tuning ensured an effective contribution of rf power to the discharge plasma and an acceptable level of matching. In the range 50–600 W of variation of the applied power and in the pressure interval 50–110 Torr in the working mixture of composition $CO_2 : N_2 : He : Xe = 1 : 1 : 3 : 0.25$, less than 5 % of the output power of the rf pump generator is reflected. A correcting inductance was installed at the other end of the electrodes for longitudinal alignment of the rf field [the field inhomogeneity along the electrodes (z axis) was less than 10 %] [10]. The rf power supplied to the discharge was defined as the difference between the incident and reflected power and measured with the help of a power meter registering the two quantities. The laser radiation power was measured by a Coherent-210 power meter.

Laser studies were carried out with the help of hybrid waveguide-unstable asymmetric confocal resonators with radiation extraction from one end. The resonators are unstable along the gap (x axis) between the electrodes and stable across it (y axis) in the waveguide mode. The advantages of the unstable resonator make it possible to attain good spatial and frequency parameters of the laser with a high gain and a large volume of the active medium, and make it possible to operate with a single (lowest) hybrid mode which fills the entire resonator volume. The main advantages of the unstable resonator also include the possibility of using only the reflective optical elements for constructing the resonator as well as for extracting radiation.

Figure 2 shows the scheme of the resonators used in the laser. The resonators are made of spherical copper mirrors with a reflectivity of 99 % at 10.6 μm extracted from the laser through a ZnSe window with an antireflective coating.

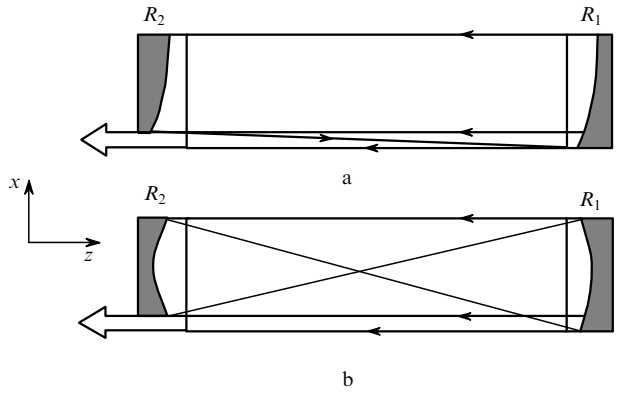

Figure 2. Scheme of confocal hybrid unstable-waveguide resonators used in a planar CO_2 laser: (a) resonator of first type, corresponding to the positive branch of the stability diagram; (b) resonator of second type, corresponding to the negative branch of the stability diagram.

The first type of the resonator, corresponding to the positive branch of the stability diagram in the 'broad' transverse direction of the discharge channel (along x axis) consists of concave and convex mirrors with radii of curvature $R_1 = 5970$ mm and $R_2 = -5152$ mm respectively. The distance between the mirrors is $L = (R_1 + R_2)/2 = 409$ mm, and the geometrical magnification $M = -R_1/R_2$ for a complete passage is equal to 1.16 in this case. The optical axis of the resonator passes along the lateral edge of the planar structure from the side opposite to the output coupling aperture of size (along x axis) $a_0 = 2a(1 - 1/M) \approx 5.5$ mm. Such an aperture corresponds to a transmission coefficient $a_0/(2a) = 0.137$ (13.7 %) of the output mirror of the resonator.

The second type of the resonator corresponds to the negative branch of the stability diagram and consists of

concave mirrors with radii of curvature $R_1 = 435.5$ mm and $R_2 = 371.5$ mm, respectively. The distance between the mirrors is $L = 403.5$ mm, and the geometrical magnification M is equal to -1.17 in this case. The optical axis of the resonator is displaced by $a(1+M)/(1-M) \approx 1.5$ mm from the core of the broad side of the planar structure from the side opposite to the output coupling aperture of size $a_0 = 2a(1+1/M) \approx 5.8$ mm, which corresponds to a transmission coefficient 14.7 % for the output mirror of the resonator.

A decided advantage of the construction is the absence of insulating lateral walls in the discharge channel, which ensures a more uniform distribution of rf voltage along the electrodes of the discharge structure and hence a higher longitudinal homogeneity of the discharge plasma than in the case when the discharge channel has insulating lateral walls (on account of the transmission line effect). The absence of the lateral walls and vertical arrangement of the discharge are also conducive for stabilising the plasma-chemical composition of the working gas mixture owing to a more intense diffusion exchange and convective replacement of the working gas mixture in the open discharge channel by the gas from the ballistic laser volume.

The electrode gap $2b = 3$ mm was chosen from the condition of a proper cooling of the working gas and low waveguide losses, as well as from the empirical dependence of the pump field frequency (40 MHz in our case) on the electrode gap, which was derived from the condition of attainment of optimal lasing conditions in the gas pressure range 50 – 120 Torr [10].

3. Results of numerical simulation

The losses associated with the extraction of radiation in an unstable finite-aperture resonator are associated with geometrical as well as diffraction effects. These losses have a quite complex and nonmonotonic dependence on the resonator geometry and an increase in the Fresnel number makes the average loss factor tend to the value defined by the geometrical optics approximation. A confocal or telescopic arrangement is usually chosen for the resonator to reduce the divergence of radiation [11 – 13].

For such a resonator consisting of mirrors with radii of curvature R_1 and R_2, the distance between the mirrors is $L = (R_1 + R_2)/2$ and the geometrical magnification is $M = -R_1/R_2$. The first type of the resonator is formed by spherical mirrors with radii of curvature $R_1 = 5970$ mm and $R_2 = -5152$ mm. The resonator length $L = 409$ mm, and the geometrical magnification $M = 1.16$ which corresponds to the positive branch of the unstable resonator. For the resonator of the second kind, the radii of curvature of the mirrors are $R_1 = 435.5$ mm and $R_2 = 371.5$ mm, $L = 403.5$ mm, and $M = -1.17$ which corresponds to the negative branch of the unstable resonator. For the geometrical optics approximation, the effective losses associated with radiation extraction after a round trip of the resonator are equal to 13.7 % and 14.7 % respectively for the above-mentioned pairs of mirrors.

The field distribution $W(x, y) = F(x)G(y)$ at the resonator output is the product of two independent functions, viz., $F(x)$ (lowest mode of the unstable resonator) and $G(y)$ (fundamental mode of the slit resonator), and has been described in detail in the literature [12, 13].

For the one-dimensional case, the field distribution $F(x)$ at the point (x_0, z) is defined by the diffraction integral

$$F(x_0) = \frac{1}{\sqrt{\mathrm{i}\lambda z}} \int_{-\infty}^{+\infty} U(x) \exp\left\{\mathrm{i}k\left[z^2 + (x - x_0)^2\right]^{1/2}\right\} \mathrm{d}x, \quad (1)$$

where $U(x)$ is the field distribution at the system input; λ is the radiation wavelength; and $k = 2\pi/\lambda$ is the wave number. Retaining the first two terms

$$\mathrm{i}k\left[z + \frac{(x - x_0)^2}{2z}\right]$$

in the expansion of the expression in the braces, we arrive at the (parabolic) Fresnel approximation. In this case, formula (1) can be presented in the form

$$F(x_0) = \frac{1}{\sqrt{\mathrm{i}\lambda z}} \exp(\mathrm{i}kz) \int_{-\infty}^{+\infty} U(x) \exp\left[\mathrm{i}\frac{\pi}{\lambda z}(x - x_0)^2\right] \mathrm{d}x. \quad (2)$$

The integral in (2) is known as the convolution of the field distribution $U(x)$ at one of the mirrors with the pulse response of the system [14]. This is equivalent to the calculation of inverse Fourier transform of the product of the transfer function of free space into Fourier transform of the transparency. Thus, the evaluation of the diffraction integral boils down to the well known Fourier transform.

The solution was found by using the method proposed by Fox and Lee. The homogeneous amplitude and phase distributions of the field at the mirror were chosen as the initial distributions. Calculations were performed with the help of the fast Fourier transform (FFT) and correspond to 640 points for a mirror with an aperture of 40 mm. Stabilisation (to within 1 %) of the ratio of the output laser power to the power of radiation incident on the output mirror served as the criterion for the formation of a stable field configuration in the resonator. The convergence of the solution (number of iterations) is nonmonotonic and depends on the Fresnel number.

Formula (2) presented above was obtained by simplifying the diffraction integral (Fresnel approximation) and under the condition that an angular aberration of $\pi/100$ is admissible [14]. This is equivalent to the condition

$$25\frac{a}{\lambda} < \left(\frac{z}{a}\right)^3, \quad (3)$$

where $2a$ is the aperture of the output mirror. In the expansion of the phase factor from Eqn (1), i.e.,

$$\left[z^2 + (x - x_0)^2\right]^{1/2} \approx z + (x - x_0)^2 \frac{1}{2z} - (x - x_0)^4 \frac{1}{(2z)^3} \quad (4)$$

the error in the first approximation, which is equal to $a^4/(2z)^3$, must be much smaller than unity.

For both types of resonators, the equivalent Fresnel number N_F^eq is defined by the expression

$$N_\mathrm{F}^\mathrm{eq} = \frac{|M - 1|}{2M^2} N_\mathrm{F},$$

where $N_\mathrm{F} = a^2/(\lambda L)$ is the Fresnel number and $a = 20$ mm. For the first resonator, we obtain $N_\mathrm{F} = 92$ and $N_\mathrm{F}^\mathrm{eq} = 5$, while for the second resonator the corresponding values are $N_\mathrm{F} = 93$ and $N_\mathrm{F}^\mathrm{eq} = 73$. The equivalent Fresnel number is

proportional to the difference in the curvature of the mirror and the curvature of the wave surface adjoining the mirror.

The resonator used by us was about 400-mm long, hence the radiation losses for the fundamental resonator mode were calculated by taking into account the next term in the expansion of the phase factor. Figure 3 shows the results of calculations for the first type of the resonator. It can be seen that the additional term in the phase factor does not have a considerable effect on the results, but its inclusion leads to a smoother dependence of 'effective' losses on the size of the output mirror (Fresnel number).

The quasiperiodic dependence of radiation losses for the first type of the resonator on the mirror aperture (and N_F^{eq}) is well known and is attributed to diffraction effects at the mirror edges (sharp edge), which lead to the emergence of undistorted reflected wave as well as an auxiliary wave generated by the mirror edge. This radiation gives rise to a wave converging at the resonator axis and influencing considerably the field structure as well as the losses, which is typical for small values of N_F^{eq}. Upon an increase in the value of N_F^{eq}, the role of diffraction at the apertures becomes less significant. This is due to a decrease in the relative diffraction variation of the reflected wave upon an enhancement of the geometrical optics transformation of wavefronts at the mirror. As the value of N_F^{eq} increases, the losses tend to their value in the geometrical optics approximation [15, 16].

For the sake of comparison, the dependence of losses on the size of the output mirror is shown in Fig. 3 for the case of a resonator with smoothed mirror edges. To attain smoothness of the edge, the reflectivity of the mirror was set to decrease from unity to zero not abruptly, but over a length of the order of 0.4 mm according to a nearly sinusoidal law. The difference in losses in this case and the geometrical optics approximation losses (for a symmetric arrangement of the output apertures, the losses will be slightly lower than in the case of geometrical optics approximation) corresponds to a displacement of the centre of gravity of the field distribution at the mirror towards the output aperture. This leads to a slight increase in the losses in comparison to the losses in the geometrical optics approximation. A displacement of the optical axis in the resonator leads to a decrease in the losses so that the losses of 14.8 % for a coupling aperture of size 5.5 mm in the mirror decrease to 14 % and 12.2 % upon a displacement of the axis by 1 mm and 2 mm, respectively.

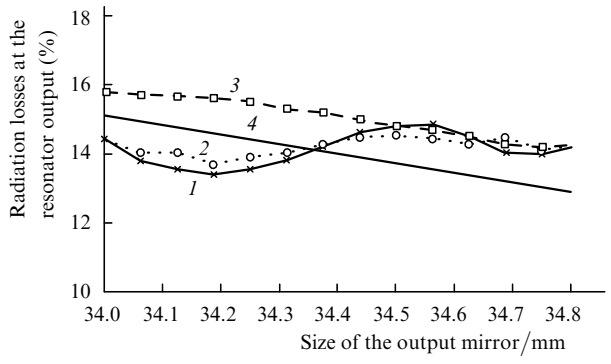

Figure 3. Dependence of the losses of radiation emerging from a resonator of the first type on the size of the output mirror by neglecting the correction in the expansion of the phase factor [curve (*1*)], and taking the correction into account [curve (*2*)], for a smooth edge of the output mirror [curve (*3*)] and in the geometrical optics approximation [curve (*4*)].

Figure 4 shows the intensity and phase distribution of the field over the output mirror aperture for the first type of the resonator. It can be seen that these distributions are quite uniform over the entire mirror aperture (and in the resonator also). If the distance between the mirrors is not optimal (i.e., if the radii of curvature of the mirrors do not match), the field phase acquires a quadratic modulation, and hence the output beam is no longer parallel. The second type of the resonator is especially sensitive in this respect on account of a larger (by an order of magnitude) curvature of the mirrors. Figure 5 shows the field intensity distribution at distances $z = 20$ and 70 mm from the output mirror. The theoretical distributions are in good agreement with the experimental results.

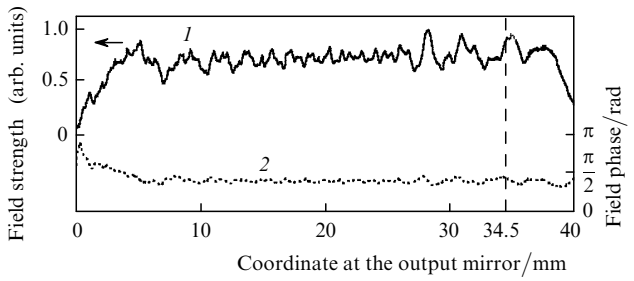

Figure 4. Field intensity [curve (*1*)] and phase [curve (*2*)] profiles at the output mirror of a resonator of the first type. The output mirror size is 34.5 mm.

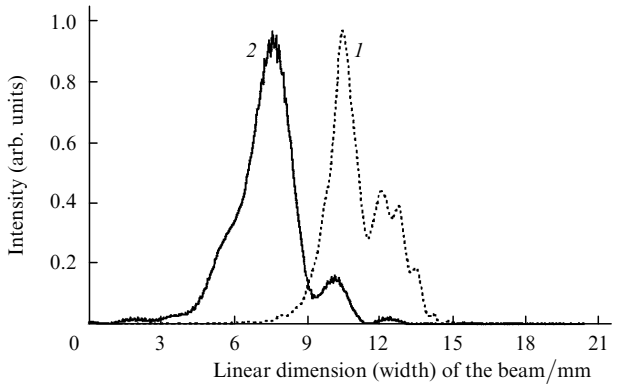

Figure 5. Intensity distribution in a laser beam along the unstable coordinate at a distance $z = 20$ [curve (*1*)] and 70 mm [curve (*2*)] from the output mirror of an optical resonator of the first type.

Figure 6 shows the results of calculation of the beam intensity distribution in the far-field zone (at the lens focus). Note that the field distribution is Gaussian, although a bit asymmetric. Consequently, the high quality of the laser beam makes it possible to use it for various purposes, including technological applications. The angular distribution in a direction perpendicular to the slit corresponds to the intensity distribution of a Gaussian beam with a waist of radius $w_0 \sim 0.7b$ (this beam waist radius corresponds to the highest coefficient of transformation of the waveguide mode to the fundamental Gaussian mode in free space), where $2b = 3$ mm, which corresponds to an angular divergence of $\theta = 2\lambda/(\pi w_0) = 6.5$ mrad at the $1/e^2$ level (or of the order of

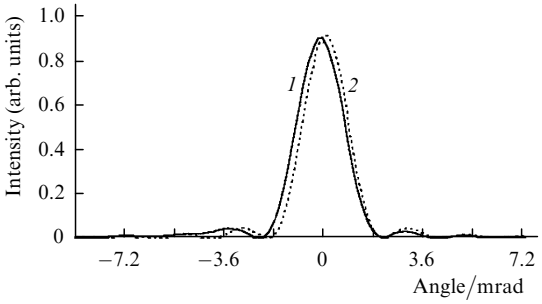

Figure 6. Distribution of the laser radiation intensity in the far-field zone along the unstable coordinate for a resonator of the first type with a coupling aperture of size 5.5 mm in the indicated direction [curve (*1*)] and for diffraction at a slit of width 5.5 mm [curve (*2*)].

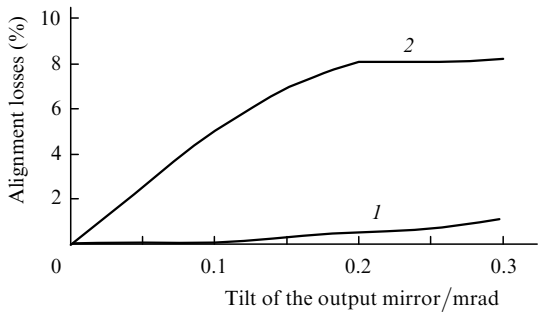

Figure 8. Dependence of the results of numerical calculations for the waveguide [curve (*1*)] and unstable [curve (*2*)] directions on the tilt (misalignment) of the output mirror in the appropriate directions for a resonator of the first kind.

4 mrad at the half-power amplitude level). According to our calculations, the diffraction divergence along the slit for an output aperture $a_0 = 5.5$ mm is about 3.5 mrad.

Waveguide losses and the losses associated with the matching of intrinsic waveguide modes with the free space modes and with mirrors constitute intrinsic losses of the waveguide resonator. The waveguide losses associated with absorption at the walls of a planar aluminium waveguide (with complex refractive index $\nu = 20 - 60\mathrm{i}$ at $\lambda = 10.6$ μm) for radiation polarised at right angles to the plane of incidence (TE- or E-wave) are estimated at a few tenths of one percent.

The dependence of losses associated with matching on the distance between the waveguide edge and the mirrors was calculated in the same way as for an unstable resonator using the FFT technique based on the Kirchhoff equation. Losses were calculated for a convex mirror ($R_1 = -5152$ mm), a concave mirror ($R_2 = 5970$ mm), and a plane mirror. The gap between the electrodes was 3 mm. The field distribution was first calculated for the fundamental waveguide mode at its output. This was followed by the calculation of field distribution at the mirror and at the waveguide input. Finally, the coefficient of coupling of the field with the field of the fundamental waveguide mode was calculated. For the sake of comparison, we carried out calculations for a concave mirror using the technique described in [17]. An almost complete agreement was observed with the solution based on the diffraction integral (Fig. 7).

We calculated the losses associated with matching depending on the precision of alignment of the concave and convex mirrors for the fundamental slit waveguide mode. The losses for the concave and convex mirrors were found to be nearly identical. Figure 8 shows the results of calculation of losses as a function of the angle of inclination of the output mirror in appropriate directions for the first type of the resonator. It can be seen that the resonator losses are more sensitive to alignment along the unstable coordinate [18].

Figure 9 shows the output laser power (numerical calculations based on Rigrod's formula taking into account the distribution losses [19]) for an output aperture 5.5×3 mm of the first type of the resonator as a function of misalignment of the highly reflecting mirror along the unstable coordinate.

Figure 10 shows the theoretical dependence of losses on the inclination of the output mirror for a resonator of

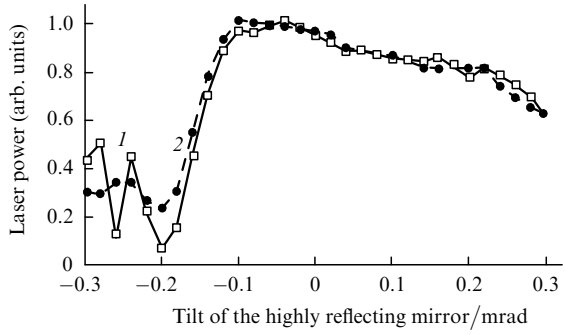

Figure 9. Variation of the output laser power (numerical calculations) for a resonator of the first type as a function of the misalignment of the highly reflecting mirror along the unstable coordinate for an output mirror with sharp [curve (*1*)] and smooth [curve (*2*)] edges.

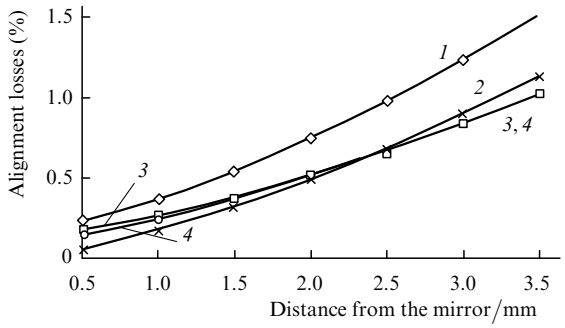

Figure 7. Dependence of the alignment losses for the fundamental mode of a waveguide resonator on the distance between the waveguide edge and the mirror for a convex [curve (*1*)], plane [curve (*2*)] and concave [curve (*3*), (*4*)] mirrors, calculated by two different methods (see text).

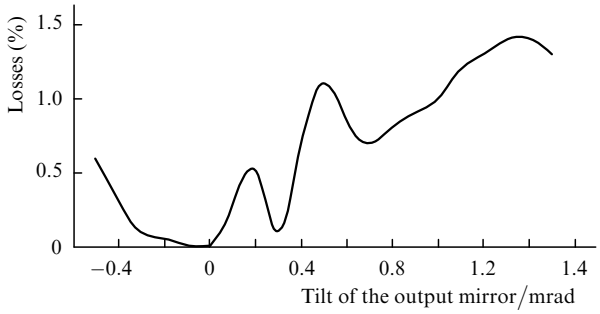

Figure 10. Results of numerical calculations along the unstable coordinate as a function of the tilt (misalignment) of the output mirror in the same direction for a resonator of the first type.

second type. It should be noted that a certain periodicity in the variation of output laser power (losses) with the inclination of the mirror was also observed in the experiments. It also follows from these investigations that on the one hand, resonators of second type are more stable (less sensitive to misalignment), while on the other hand they are very sensitive to departure of the resonator length from the optimal value (Fig. 11) on account of a considerable variation of the radiation losses (transmission coefficient of the output mirror). It can be seen that a more precise matching of the resonator length with the radii of curvature of the mirrors is required for resonators of the second kind [19]. It should also be noted that for an optimal resonator length, the radiation losses calculated by wave analysis are slightly lower than those obtained from geometrical optics approximation, and amount to 14.7 %.

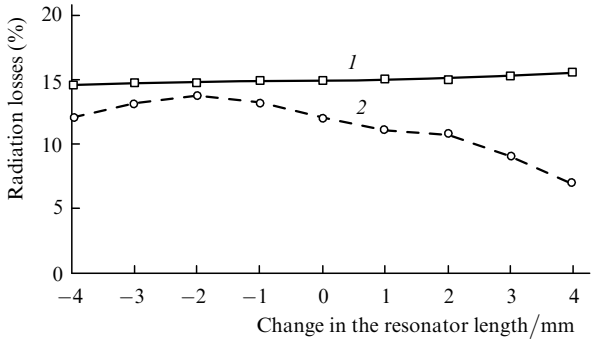

Figure 11. Radiation losses for a resonator of the first [curve (*1*)] and second [curve (*2*)] types as a function of the departure of the resonator length from the optimal value.

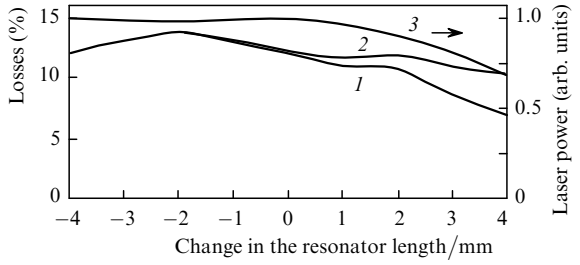

Figure 12. Dependence of the calculated aperture losses [curve (*1*)] and total losses [curve (*2*)], as well as the output power of a laser with a resonator of the second type [curve (*3*)] on the departure of the resonator length from the optimal value.

Figure 12 shows the results of calculations of aperture losses and total losses, as well as the output power of a laser with a resonator of the second kind, as functions of the departure of the resonator length from the optimal value.

4. Experimental results

4.1 Parameters of the rf discharge

Figure 13 shows a family of curves illustrating the mean-square value of the voltage U_{dis} across the electrodes as a function of the power W_{in} supplied to the rf discharge for various fixed values of pressure p of the working gas mixture. These dependences lead, albeit indirectly, to an estimate of the reduced electric field strength E/N in the plasma discharge (N is the number density of particles in

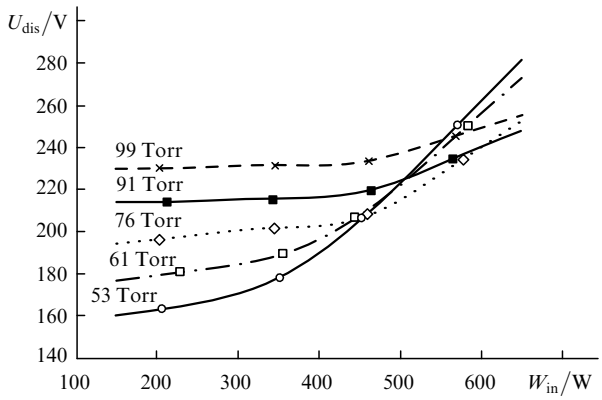

Figure 13. Dependence of the voltage U_{dis} across the electrodes on the power W_{in} supplied to the rf discharge under various pressures of the working gas mixture $CO_2:N_2:He:Xe = 1:1:3:0.25$ for an electrode gap of 3 mm and rf field frequency 40 MHz.

the gas mixture), characterising the efficiency of transformation of the input power into coherent radiation.

Figure 14 shows the dependence of the supplied power density W_{in}/S (where S is the area of the working surface of electrodes covered by the discharge) on the working gas pressure for the case of rf discharge in the normal current density regime. The quantity W_{in}/S was measured at the instant when the discharge covered the electrode area completely, and was found to be equal to 1–4 W cm^{-2} for the rf discharge in the normal current density regime under a working gas pressure $p = 50 - 110$ Torr. These data were obtained for the first time and are important for optimisation and scaling of generation parameters of high-power planar CO_2 lasers.

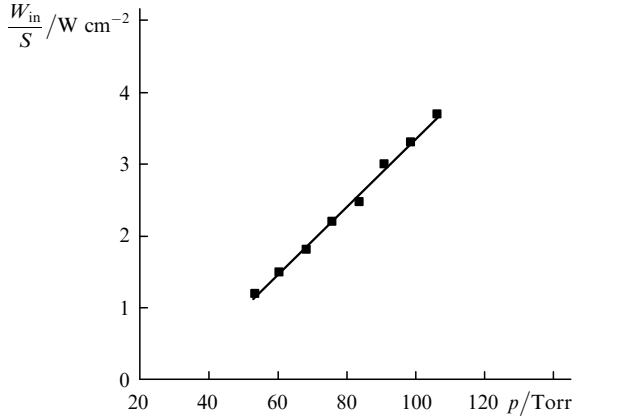

Figure 14. Dependence of the applied power density W_{in}/S on pressure p of the working gas mixture $CO_2:N_2:He:Xe = 1:1:3:0.25$ for an rf discharge under normal current density and rf field frequency 40 MHz.

4.2 Energy parameters of the laser

Figure 15 shows the dependence of the output power W_{out} of a planar CO_2 laser on the pressure p of the working gas mixture for an optical resonator of the first kind. The dependence was obtained for a fixed rf power $W_{in} = 600$ W supplied to the discharge.

Figure 16 illustrates the dynamic potentialities of the planar laser. It shows the dependence of W_{out} on the supplied power W_{in} for the case when the chosen working gas pressure is optimal from the point of view of obtaining the highest lasing power. Experiments show that the output

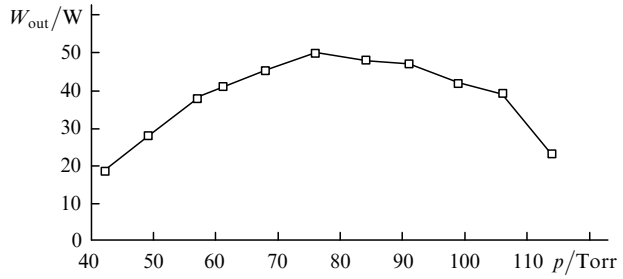

Figure 15. Dependence of the output laser power W_{out} on pressure p of the working gas mixture $CO_2:N_2:He:Xe = 1:1:3:0.25$ for $W_{in} = 600$ W and rf field frequency 40 MHz for an optical resonator of the first type.

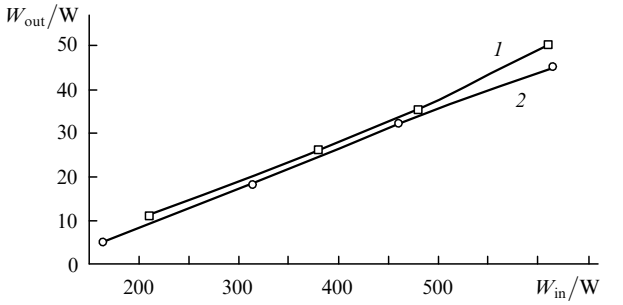

Figure 16. Dependence of the output laser power W_{out} on the power W_{in} supplied to the rf discharge for an optical resonator of the first [curve (*1*)] and second [curve (*2*)] types for a pressure $p = 76$ Torr of the working gas mixture $CO_2:N_2:He:Xe = 1:1:3:0.25$ for an rf field frequency of 40 MHz.

power is almost the same for both types of resonators and that the laser does not attain the saturation regime. Moreover, modulation of W_{in} (up to 100 % at a frequency of 50 Hz) for a constant mean supplied power, which is equivalent to doubling of the pulse power, also led to doubling of the laser pulse power for a constant mean output power of 50 W.

Under the conditions of our experiment, the maximum possible power W_{in} supplied to the rf discharge was 600 W. This limitation did not allow us to demonstrate fully the potentialities as regards the attainable output power W_{out} and the efficiency of the laser. However, our investigations of the output power and spatial characteristics of the planar CO_2 laser radiation as well as the rf-discharge plasma parameters led to a number of peculiarities that are apparently characteristic of planar lasers irrespective of the structural design of the electrode–waveguide system, optical resonator scheme and rf pump parameters.

In our experiments, the maximum specific power supplied to the discharge plasma did not exceed 12.5 W cm^{-3}. Numerical calculations and our earlier investigations [10] of the waveguide laser under conditions close to those of our experiment show that the linear growth of the output power is preserved for an energy input of 55.5 W cm^{-3} also. All this indicates that an output power $W_{out} \approx 250$ W is really attainable in such a model of planar laser.

Figure 17 shows the dependence of the output power of a laser with a resonator of the second type on the misalignment of the highly reflecting mirror along the unstable coordinate. The same figure also shows the results of numerical calculations which are found to be in good agreement with the experimental data.

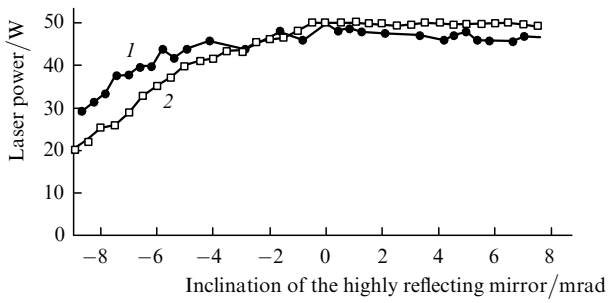

Figure 17. Experimental [curve (*1*)] and theoretical (numerically calculated) [curve (*2*)] dependences of the output laser power on the misalignment of the highly reflecting mirror along the unstable coordinate for an optical resonator of the second type.

4.3 Spatial parameters of laser radiation

Figure 18 shows the laser beam dimensions in two mutually orthogonal directions (along and across the discharge gap) as functions of the distance z from the output mirror for an optical resonator of the first kind. The beam size was determined at the 10 %-level of the maximum intensity. The radiation divergence along the waveguide and the unstable directions in this resonator was 7.5 and 4 mrad respectively, which is in good agreement with the diffraction divergence $\theta = 2\lambda/(\pi w_0)$ estimated for an aperture 3×5.5 mm of the output aperture.

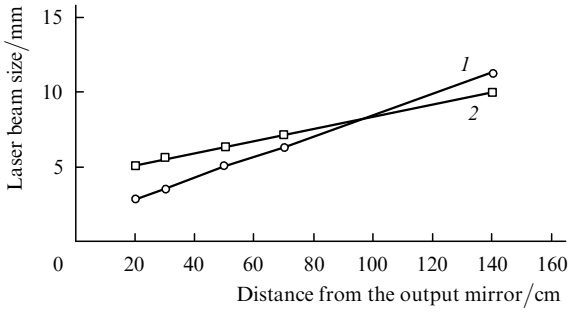

Figure 18. Dependence of the laser beam size along the waveguide direction [curve (*1*)] and the unstable direction [curve (*2*) on the distance from the output mirror in a resonator of the first type for an angle $\theta = 7.5$ mrad [curve (*1*)] and 4 mrad [curve (*2*)] in which over 90 % of the beam energy is concentrated.

Figure 19 shows the experimental distributions of the laser radiation intensity along the unstable coordinate at distances 20 and 70 cm from the output resonator mirror, obtained by drilling a hole in an organic glass by a laser beam.

5. Conclusions

We have constructed and investigated a planar waveguide CO_2 laser with an all-metal electrode–waveguide structure (without insulating lateral walls), excited by an rf discharge at a frequency of 40 MHz with diffusion cooling. We have studied in detail the dependence of the energy and spatial parameters of cw laser radiation on the input rf power (up to 600 W) and pressure of the working gas mixture (up to 110 Torr). The electrical characteristics of the discharge are studied as well as the parameters and conditions of its burning in the laser channel.

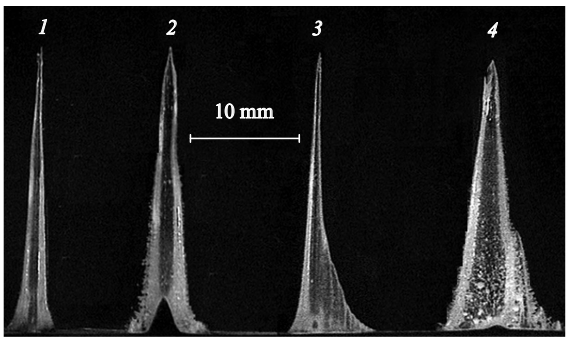

Figure 19. Experimental intensity profiles of the output laser beam along the unstable coordinate obtained for an organic glass for optical resonators of the second [curve (*1*), (*2*)] and first [curve (*3*), (*4*)] types at distances $z = 20$ [curve (*1*), (*3*)] and 70 mm [curve (*2*), (*4*)] from the output mirror.

In the single-mode generation, a cw laser power ~ 50 W was attained at an efficiency of about 10 % for a nearly diffractional divergence of radiation (4–7 mrad). The voltage across the electrodes ($U_{dis} = 150 - 300$ V) and the input power density ($W_{in}/S = 1 - 4$ W cm^{-2}) were measured for an rf discharge in the normal current density regime for a working gas pressure of 40–110 Torr. These experimental results have been obtained for the first time and are important for optimisation and scaling of generation parameters of high-power planar CO_2 lasers. The output laser power increases linearly with the applied rf power. Calculations based on the experimental data indicate that an output laser power exceeding 200 W can be attained without any significant superheating of the active medium.

Two schemes of confocal hybrid unstable-waveguide resonators (corresponding to the positive and negative branches of the stability diagram) with a geometrical magnification $M \approx 1.16$ were studied in a planar CO_2 laser both experimentally and by numerical simulation.

A comparative analysis of quantitative and qualitative characteristics of the stability and precision of alignment of mirrors, as well as power and spatial structure of laser radiation, was made for both kinds of resonators.

We have worked out recommendations for optimising the modal structure and output energy characteristics of laser radiation for various schemes of optical resonators, as well as recommendations for their practical applications. It is found that for an optical resonator corresponding to the negative branch of the stability diagram, the misalignment of mirrors leading to a 50 % decrease in the output laser power is 0.02 rad, while for the positive branch of the stability diagram, the corresponding misalignment is 100 times smaller. Apparently, the resonator corresponding to the negative branch is an order of magnitude more sensitive to the violation of confocal arrangement of mirrors as a result of an increase in its length.

The results obtained experimentally and by numerical simulation are in good accord with each other and with the other available results of measurements of output characteristics of PWL radiation and rf discharge parameters for various constructions of CO_2 lasers in a wide range of specific energy inputs, working gas pressures and rf-excitation frequencies.

The advantages of the CO_2 laser with an all-metal electrode–waveguide structure include low cost of the material (aluminium), convenience of surface processing, possibility of direct cooling of all the waveguide walls, the presence of air gaps in the discharge channels for ensuring the shortest contact with the ballast gas volume (thus partially solving problems of plasma chemistry and life span of the working mixture in the sealed regime), and a higher rf discharge homogeneity along the metal construction as compared to the insulator one.

Further progress in the field of rf-pumped diffuse planar CO_2 lasers can be made by studying the conditions of passage of current at the boundaries of the rf-discharge plasma with the electrodes, by increasing the rate of heat removal from the discharge chamber walls, and by solving the problems associated with the choice of a particular hybrid unstable-waveguide resonator scheme.

The results of this research can be used for designing and developing 1-kW CO_2 lasers operating both in the cw and repetitively-pulsed regimes with laser pulse durations of 10–100 μs, pulse repetition rates of up to 5 kHz, and peak power ~ 10 kW.

Acknowledgements. This work was supported by the Russian Foundation for Basic Research (Grant No. 05-02-17624).

References

1. Jackon P.E., Baker H.J., Hall D.R. *Appl. Phys. Lett.*, **54** (20), 1950 (1989).
2. Colley A.D., Baker H.J., Hall D.R. *Appl. Phys. Lett.*, **61** (2), 136 (1992).
3. Kuznetsov A.A., Ochkin V.N., Udalov Yu.B., Witteman W.J. *Laser Phys.*, **4** (6), 1106 (1994).
4. Leont'ev V.G., Sukhanova N.P., Shushkanov A.F. *Kvantovaya Elektron.*, **21**, 931 (1994) [*Quantum Electron.*, **24**, 869 (1994)].
5. Mineev A.P., Nefedov S.M., Pashinin P.P. *Techn. Dig. CLEO/Europe'96* (Hamburg, 1996) CTuN6.
6. Dutov A.I., Evstratov I.Yu., Ivanova V.N., Kuleshova A.A., Motovilov S.A., Novoselov N.A., Semenov V.E., Sokolov V.N., Yur'ev M.S. *Kvantovaya Elektron.*, **23**, 499 (1996) [*Quantum Electron.*, **26**, 484 (1996)].
7. Lapucci A., Labate A., Rossetti F., Mascalchi S. *Appl. Opt.*, **35**, 3185 (1996).
8. Mineev A.P., Nefedov S.M., Pashinin P.P. *Proc. SPIE Int. Soc. Opt. Eng.*, **3686**, 35 (1999).
9. Mineev A.P., Nefedov S.M., Pashinin P.P. *Proc. SPIE Int. Soc. Opt. Eng.*, **5137**, 288 (2003).
10. Lipatov N.I., Mineev A.P., Pashinin P.P., Prokhorov A.M. *Kvantovaya Elektron.*, **16**, 938 (1989) [*Sov. J. Quantum Electron.*, **19**, 610 (1989)].
11. Sigmen A.E. *Proc. IERE*, **53**, 318 (1965).
12. Maitland A., Dunn M.H. *Laser Physics* (Amsterdam: North-Holland, 1969; Moscow: Nauka, 1978).
13. Svelto O. *Principles of Lasers* (New York: Plenum Press, 1998; Moscow: Mir, 1979).
14. Papoulis A. *Systems and Transforms with Applications in Optics* (New York: McGraw-Hill, 1968; Moscow: Mir, 1971).
15. Anan'ev Yu.A. *Opticheskie rezonatory i lazernye puchki* (Optical Resonators and Laser Beams) (Moscow: Nauka, 1990).
16. Ishchenko E.F. *Otkrytye opticheskie rezonatory* (Open Optical Cavities) (Moscow: Sov. Radio, 1980).
17. Avrillier S., Verdonck J. *J. Appl. Phys.*, **48**, 4937 (1978).
18. Kuznetsov A.A., Ochkin V.N., Ksin J. *Preprint FIAN No. 62* (Moscow, 1997).
19. Balakin S.V., Leont'ev V.G., Rakhvalov V.V., Stepanov V.A., Shishkanov E.F., Yukhimuk A.A. *Zh. Prikl. Spektr.*, **54** (6), 931 (1991).